

1 Production, characterization and application of an alginate lyase,  
2 AMOR\_PL7A, from hot vents in the Arctic Mid-Ocean Ridge  
3

4 Kiira S. Vuoristo<sup>1\*</sup>, Lasse Fredriksen<sup>1</sup>, Maren Oftebro<sup>1</sup>, Magnus Ø. Arntzen<sup>1</sup>, Olav A. Aarstad<sup>3</sup>, Runar Stokke<sup>2</sup>, Ida H.  
5 Steen<sup>2</sup>, Line Degn Hansen<sup>1</sup>, Reidar B. Schüller<sup>1</sup>, Finn L. Aachmann<sup>3</sup>, Svein J. Horn<sup>1</sup>, Vincent G.H. Eijsink<sup>1\*</sup>

- 6 1. Faculty of Chemistry, Biotechnology and Food Science, Norwegian University of Life Sciences (NMBU), P.O. Box  
7 5003, N-1432 Aas, Norway
- 8 2. Department of Biological Sciences and KG Jebsen Centre for Deep Sea Research, University of Bergen, N-5020  
9 Bergen, Norway
- 10 3. Department of Biotechnology and Food Science, NTNU Norwegian University of Science and Technology, Sem  
11 Sælands vei 6/8, N-7491 Trondheim, Norway
- 12

---

<sup>1</sup> \* Corresponding authors Kiira S. Vuoristo [kiira.vuoristo@nmbu.no](mailto:kiira.vuoristo@nmbu.no) and Vincent G.H. Eijsink [vincent.eijsink@nmbu.no](mailto:vincent.eijsink@nmbu.no)

## 13 Abstract

14 Enzymatic depolymerization of seaweed polysaccharides is gaining interest for the production of functional  
15 oligosaccharides and fermentable sugars. We describe a thermostable alginate lyase belonging to Polysaccharide Lyase  
16 family 7 (PL7), which can be used to degrade brown seaweed, *Saccharina latissima*, at conditions also suitable for a  
17 commercial cellulase cocktail (Cellic CTec2). This enzyme, AMOR\_PL7A, is a  $\beta$ -D-mannuronate specific (EC 4.2.2.3) endo-  
18 acting alginate lyase, which degrades alginate and poly-mannuronate within a broad range of pH, temperature and  
19 salinity. At 65 °C and pH 6.0, its  $K_m$  and  $k_{cat}$  values for sodium alginate are 0.51 +/- 0.09 mg/mL and 7.8 +/- 0.3 s<sup>-1</sup>  
20 respectively. Degradation of seaweed with blends of Cellic CTec2 and AMOR\_PL7A at 55 °C in seawater showed that the  
21 lyase efficiently reduces viscosity and increases glucose solubilization. Thus, AMOR\_PL7A may be useful in development  
22 of efficient protocols for enzymatic seaweed processing.

## 23 Keywords

24 Alginate lyase, Brown seaweed, *Saccharina latissima*, Biorefining, PolyM, Salt tolerance

## 25 Introduction

26 *Saccharina latissima*, better known by its common name sugar kelp, is a widely abundant brown seaweed (macroalgae)  
27 in Norwegian coastal areas. *S. latissima* contains up to 40 % alginate of its dry weight depending on season and depth<sup>12</sup>.  
28 In Norway, exploitation of brown seaweed has so far largely been based on harvesting of natural biomass and production  
29 of valuable compounds such as alginate<sup>3</sup>. In recent years, new possibilities have opened within industrialized multi-trophic  
30 aquaculture, where seaweeds are grown in close proximity to salmon farms<sup>4</sup>. In addition to alginate, *S. latissima* is rich in  
31 polysaccharides such as cellulose, laminarin, and fucoidan, and also contains considerable amounts of mannitol<sup>5</sup>. Because  
32 of this composition, brown seaweed may be utilized for biofuel production<sup>6,7</sup> or other fermentative production processes  
33 such as the production of single cell protein<sup>8</sup>. Considering the compositional complexity, complete saccharification of  
34 brown seaweed requires a multitude of enzymes. Key enzymes include cellulases and alginate lyases, because they

35 together release a considerable amount of the available sugar<sup>9</sup> and because the viscosity reducing effect of alginate lyase  
36 has a general positive effect on enzymatic degradability<sup>10,11</sup>.

37 Alginate lyases, characterized as either mannuronate (EC 4.2.2.3) or guluronate (EC 4.2.2.11) lyases, catalyze  
38 depolymerization of alginate, a co-polymer consisting of the uronic acids  $\beta$ -D-mannuronate (M) and its C5 epimer  $\alpha$ -L-  
39 guluronate (G). In alginates, these monomers occur as homopolymeric blocks of consecutive M-residues (polyM) or  
40 consecutive G-residues (polyG), or in heteropolymeric blocks of alternating M and G-residues (polyMG). According to the  
41 Carbohydrate-Active Enzymes database (CAZy), alginate lyases occur in several families of polysaccharide lyases (PL). To  
42 date, alginate lyases are found in PL families 5, 6, 7, 14, 15, 17, and 18 and most of them work endolytically<sup>12</sup>.  
43 Polysaccharide lyases (EC 4.2.2.-) are active on uronic acid containing polysaccharides and cleave the substrate by a  $\beta$ -  
44 elimination reaction, which generates a new reducing end and an unsaturated uronic acid at the new non-reducing end  
45<sup>13</sup>. Alginate lyases acting mainly on the M-M bond or G-G bond are classified as poly-mannuronate (polyM) lyases, poly-  
46 guluronate (polyG) lyases, respectively<sup>12</sup>. Due to the enzymatic formation of a double bond between C4 and C5, the  
47 unsaturated residues originating from guluronic acid (G) or mannuronic acid (M) are identical. This urinate, 4-deoxy-L-  
48 erythro-hex-4-enopyranosyluronate, is often shown as  $\Delta$  in illustrations<sup>12,14</sup>.

49 Alginate lyases, including commercially available ones, typically have a lower temperature optimum than commercial  
50 cellulase cocktails. Hydrolysis of seaweed must therefore be done in two phases, at two different temperatures, requiring  
51 long processing times<sup>9</sup>, while the low temperature processing step with the alginate lyase increases the risk of bacterial  
52 contamination. Here, we describe the cloning and characterization of a novel, thermostable alginate lyase (AMOR\_PL7A)  
53 whose gene was retrieved from a metagenomic dataset collected from the Arctic Mid-Ocean Ridge (AMOR). Furthermore,  
54 we show that AMOR\_PL7A promotes saccharification of seaweed by the commercial enzyme cocktail Cellic CTec2 in a  
55 single step reaction.

## 56 Material and methods

### 57 Sampling, DNA extraction and sequencing

58 A sample of unbleached Norway spruce (*Picea abies*) that had been pretreated by sulfite-pulping using the BALI™ process  
59 <sup>15,16</sup> at Borregaard AS (Sarpsborg, Norway), was incubated for one year in ~70°C hot sediments at the Arctic Mid-Ocean  
60 Ridge (AMOR), 570 meters below sea level<sup>17,18</sup>. In short, one gram of spruce material was mixed with approximately 16 ml  
61 of sediment sampled at the site and placed in the middle chamber of a titanium incubator with three vertically aligned  
62 chambers of 2.5 cm in length, a volume of 16 ml and 1 mm pores. DNA was extracted from 4.6 grams of material and 1.8  
63 µg of DNA was submitted for sequencing. Further details of the substrate and the sampling procedure, as well as the  
64 procedures used for DNA extraction and sequencing have been described elsewhere <sup>19</sup>.

### 65 Filtering, assembly and ORF-prediction

66 Raw Illumina MiSeq 300 paired-end reads were filtered and assembled using the CLC genomics workbench (Qiagen,  
67 v.9.5.3), with CLC default parameters for filtering (quality 0.05, length min. 40 and max. 1000 nucleotides) and assembly  
68 (automatic k-mer size and bubble size). Before filtering, one nucleotide was removed from terminal read ends. The  
69 minimum contig length was set to 1000 bases, with scaffolding enabled. Open reading frames were predicted using the -  
70 *p meta* option in Prodigal v.2.6.3 <sup>20,21</sup> for metagenomics datasets. A full description of the resulting dataset will be  
71 published elsewhere.

72 The metagenomic data, which were generated for the discovery of cellulolytic enzymes, were also mined for putative  
73 endo-type lyases from polysaccharide lyase family 7 (PL7) using dbCAN (csbl.bmb.uga.edu/dbCAN)<sup>22</sup>. This analysis resulted  
74 in the identification of a 783 bp gene encoding a putative PL7, here named *amor\_PL7A* (See Figure S1 for the protein  
75 sequence). The AMOR\_PL7A amino acid sequence was Blasted against the PDB database (rcsb.org) and submitted to the  
76 Phyre2 server ([www.sbg.bio.ic.ac.uk/phyre2](http://www.sbg.bio.ic.ac.uk/phyre2);<sup>23</sup>) to investigate similarities to known alginate lyases and to check for  
77 occurrence of expected active site residues. Lipop analysis <sup>24</sup> indicated a signal peptidase II cleavage site between residues  
78 24-25, suggesting that AMOR\_PL7A is a lipoprotein anchored to the cell membrane via a cysteine at position 25. The  
79 sequence of AMOR\_PL7A has been submitted to GenBank under accession number MH727998.

## 80 Sequence analysis

81 Sequence alignments were produced in MEGA v.7<sup>25</sup> using the Muscle algorithm<sup>26</sup> and the aligned sequences were  
82 visualized using ESPript 3<sup>27</sup>. To infer phylogenetic placement of AMOR\_PL7, a pre-computed alignment of PL7 was  
83 downloaded from the dbCAN server and aligned with additional PL7 sequences as identified by using the EMBL-EBI  
84 HMMER biosequence analysis<sup>28</sup>. Only sequences sharing the conserved amino acids of the active site (Fig. S1) were  
85 considered and aligned using mafft-linsi<sup>29,30</sup>. In total, 161 sequences were used for construction of a phylogenetic tree  
86 using IQTREE<sup>31</sup>.

## 87 Cloning, expression and purification of AMOR\_PL7A

88 The *amor\_PL7A* gene (codon-optimized for *Escherichia coli* expression) was synthesized by Genscript (Piscataway, NJ, USA)  
89 and a gene fragment comprising bp 76-783 (omitting the predicted 24 amino acid signal peptide and the cysteine residue  
90 at position 25) was amplified by PCR using the Q5 DNA polymerase (New England Biolabs, Ipswich, Massachusetts, USA)  
91 and forward and reverse primers 5'TTAAGAAGGAGATATACTATGAATAGCGACGACGGTCTGCT3' and  
92 5'AATGGTGGTGATGATGGTGCCTCGTAATAATACTTCAGGCTCTTAAAT3' (Eurofins, Ebersberg, Germany), respectively.  
93 The resulting PCR product encodes for a protein with a C-terminal hexaHis-tag and was cloned into the pNIC-CH expression  
94 vector (AddGene, Cambridge, Massachusetts, USA) by Ligation-Independent cloning<sup>32</sup>, as described previously<sup>19</sup>.  
95 Transformed OneShot *E. coli* TOP10 cells (Invitrogen, Carlsbad, California, USA) were propagated, plasmids were isolated  
96 and the sequence of *amor\_PL7A* was confirmed by Sanger sequencing (GATC, Konstanz, Germany), after which a correct  
97 plasmid was transformed to OneShot BL-21 Star™ (DE3) *E. coli* cells for protein expression, all as described previously<sup>19</sup>.  
98 For expression, cells were grown in Terrific Broth (TB) supplemented with 50 µg/mL kanamycin at room temperature,  
99 overnight, using a Harbinger system (Harbinger Biotechnology & Engineering, Markham, Canada). Protein expression was  
100 then induced by adding isopropyl-β-D-thiogalactopyranoside (IPTG) to a final concentration of 0.2 mM, followed by further  
101 incubation at room temperature for 24 h. Cell pellets were collected by centrifugation at 5,000 *g*, T = 4 °C, for 15 minutes  
102 using a Beckman Coulter Avanti J-26S XP centrifuge (Brea, California, USA). The cell pellet was placed at -80 °C for 1 hour  
103 to promote cell lysis. After thawing, the cells were resuspended in 50 mM Tris-HCl (pH 8.0) containing 500 mM NaCl and  
104 5 mM imidazole, and sonicated on ice using a Vibracell sonicator (Sonics & Materials Inc., Newtown, Connecticut, USA)

105 with 5 seconds on/off pulses for 3 minutes at 30% amplitude. After removal of cell debris by centrifugation at 15,000 *g* for  
106 15 minutes, the supernatant was filtered using a 0.45  $\mu\text{m}$  syringe filter (Sarstedt, Nümbrecht, Germany). The resulting cell-  
107 free protein extract was then used for purification of AMOR\_PL7A by immobilized metal affinity chromatography (IMAC)  
108 using an Äkta pure chromatography system and a  $\text{Ni}^{2+}$  affinity HisTrap™ HP 5 mL column (GE HealthCare, Chicago, USA).  
109 Elution was achieved by applying a linear gradient of 5-500 mM imidazole in 50 mM Tris-HCl (pH 8.0), 500 mM NaCl. After  
110 analysis of protein-containing fractions by SDS-PAGE (Bio-Rad, Hercules, California, USA) (Figure S2), fractions containing  
111 AMOR\_PL7A were combined and the resulting solution was concentrated using a 3,000 MWCO Vivaspin ultrafiltration  
112 tube (Sartorius, Göttingen, Germany), with concomitant buffer exchange to 20 mM sodium acetate, pH 6.0, 300 mM NaCl.  
113 For determination of the protein concentrations, the absorbance at 280 nm was recorded with a Biophotometer  
114 (Eppendorf, Hamburg, Germany) and converted to a concentration using the theoretical extinction coefficient  
115 ([web.expasy.org/protparam](http://web.expasy.org/protparam)) of AMOR\_PL7A. Solutions with purified protein were stored at 4°C.

## 116 Activity assays

117 The activity of AMOR\_PL7A was quantified either by determining production of reducing sugar equivalents using the 3,5-  
118 dinitrosalicylic acid (DNS) reagent<sup>33</sup> or by following double bond formation through monitoring absorbance at 235 nm.  
119 Absorbance at 235 nm was converted to product concentration using an extinction coefficient of  $6150 \text{ M}^{-1}\text{cm}^{-1}$ <sup>34</sup> and a  
120 path length of 0.56 cm (200  $\mu\text{L}$  reaction volume in microtiter plates). Enzyme reactions were carried out in triplicates and  
121 the values presented below represent the mean  $\pm$  standard deviation. All reported buffer pHs were measured at 65 °C.  
122 Note that while the pH of sodium acetate buffer is almost independent of temperature, the pH of Tris-HCl buffer with a  
123 pH of 7.0 at room temperature is approximately 6.0 at 65 °C.

## 124 Dinitrosalicylic acid (DNS) assay for determination of reducing sugars

125 The optimal temperature for the enzyme was determined using the DNS method for product quantitation<sup>33</sup>. Reaction  
126 mixtures contained 25.4 nM AMOR\_PL7A in 50 mM sodium acetate (NaAc) buffer containing 500 mM NaCl (pH 6.0) and  
127 1% (w/v) standard sodium alginate from Sigma Aldrich ( $F_G = 0.44$ ,  $M_w = 107.9 \pm 2.7 \text{ kDa}$ ) and the reaction mixtures were  
128 incubated at different temperatures (37 °C to 100 °C) for up to 50 min. Samples were taken at regular intervals and  
129 subjected to boiling for 5 minutes. Samples were then mixed with two volumes of DNS reagent, followed by boiling for 15

130 minutes. Subsequently, the absorbance was measured at 540 nm using a Synergy H4 Microplate reader (Biotek  
131 Instruments Inc, Winooski, USA). Standard curves were made using guluronic acid at concentrations ranging from 0.09 to  
132 1.80 mg/mL. The linear regions of the obtained progress curves were used to determine initial velocities.

### 133 Monitoring the formation of double bonds

134 For determination of the pH optimum, kinetic measurements and assessment of thermostability, enzyme activity was  
135 assessed by recording the change in absorbance at 235 nm<sup>35</sup>. Standard reactions contained 12.7 nM AMOR\_PL7A in 50  
136 mM Tris-HCl, pH 6.0, containing 500 mM NaCl and 0.5 % (w/v) sodium alginate. Reactions were set up in triplicates and  
137 product formation was monitored in real time using a Synergy H4 Microplate reader (Biotek). Samples were incubated for  
138 up to 60 minutes at 65°C with continuous stirring in between absorbance measurements at 235 nm with one-minute  
139 intervals. The linear regions of the progress curves were used to determine initial velocities.

### 140 pH optimum and salt tolerance

141 The pH optimum of AMOR\_PL7A was investigated using the conditions described above for determination of absorbance  
142 at 235 nm, with varying buffers covering a pH range of 4.2 to 9.3, either 50 mM NaAc (pH 4.2-5.8), 50 mM Tris-HCl (pH  
143 6.0-6.9) or 50 mM Glycine-NaOH (pH 7.9-9.3) (Nb. pH measured at 65 °C). For testing the effects of salinity, the standard  
144 50 mM Tris-HCl buffer, pH 6.0, was supplied with 0 to 2 M NaCl. Seawater (pH 6.8 at 65 °C) was obtained from Norsk  
145 Institutt for Vannforskning (NIVA), Drøbak, Norway, and was collected from 60 m depth in the Oslo Fjord and a  
146 temperature of 7.6°C. Seawater salinity was measured with a Sal-Bta salinity probe (Vernier, Beaverton, USA) and  
147 corresponded to approximately 430 mM NaCl.

### 148 Determination of Michaelis-Menten enzyme kinetics

149 Steady-state kinetic constants,  $K_M$  and  $V_{max}$ , at 65°C, were calculated by direct fitting of experimental data to the Michaelis–  
150 Menten equation. Data points were collected from reactions with sodium alginate at concentrations ranging from 0.1 to  
151 9 mg/mL, containing 12.7 nM enzyme in 50 mM Tris-HCl, pH 6.0, and 500 mM NaCl. Enzyme activity was measured by  
152 recording the change in absorbance at 235 nm and all progress curves used for rate determination were linear. Enzyme

153 rates were calculated by dividing the linear increase in the concentration of saturated ends, calculated as described above,  
154 by time.

#### 155 Thermostability

156 Thermostability was determined by pre-incubating the enzyme (0.1  $\mu$ M) in 50 mM Tris-HCl, pH 6.0, and 500 mM NaCl  
157 without the substrate at 65°C for 0 to 24 hours before running an activity assay using standard conditions (50 Tris HCl, pH  
158 6.0, 500 mM NaCl, 65°C), with product monitoring at 235 nm.

159 For determination of the apparent protein melting temperatures, we used a Nano-Differential Scanning Calorimeter III  
160 (Calorimetry Sciences Corporation, Lindon, USA). Protein samples were dialyzed over night at 4°C against 50 mM sodium  
161 acetate pH 6.0 containing either 50 or 500 mM NaCl, or against pure unbuffered seawater. The dialyzed protein samples  
162 (final concentration adjusted to 1.3 mg/mL) and samples of dialysis buffer, used for recording baselines, were degassed  
163 prior to the DSC experiments. The scan rate was 1°C/minute and the temperature range was 20-100°C. The data were  
164 analyzed using the NanoAnalyze software (tainstruments.com).

#### 165 Substrate specificity

166 The substrate specificity of AMOR\_PL7A was investigated using polyM ( $M_w = 275$  kDa,  $F_G = 0.0$ ,<sup>36</sup>), polyG (DPn =20,  $F_G =$   
167  $0.93$ ,<sup>1</sup>) or polyMG ( $M_w = 275$  kDa,  $F_G = 0.46$ ,  $F_{GG} = 0.0$ <sup>37</sup>) as substrate. The reactions were performed in 50 mM Tris-HCl,  
168 pH 6.0, containing 250 mM NaCl, 12.7 nM enzyme and 0.5% (w/v) substrate. Products were analyzed by High Performance  
169 Anion Exchange Chromatography (HPAEC) for qualitative analysis and with the DNS method for quantification. Preparation  
170 of alginate oligomers for product identification, by fractionation of alginate hydrolysates on SEC columns, has been  
171 described previously by Aarstad et al.<sup>14</sup>.



172 Chromatographic product analysis

173 Samples were passed through a 0.22  $\mu\text{m}$  filter prior to chromatographic analysis. Analysis of monosaccharides and  
174 mannitol was done using a Dionex Ultimate 3000 (Sunnyvale, California, USA) HPLC system equipped with a refractive  
175 index detector and a 300  $\times$  7.8 mm Rezex ROA-Organic Acid H+ analytical column fitted with a cation-H cartridge guard  
176 column, operated at 65  $^{\circ}\text{C}$  with 5 mM  $\text{H}_2\text{SO}_4$  as the mobile phase, with a flow rate of 0.6 mL/min. Glucose and mannitol at  
177 concentrations ranging from 0.50 to 10 g/L were used as calibration standards. Analysis of oligosaccharides by high-  
178 performance anion exchange chromatography (HPAEC) was done using an ICS3000 system from Dionex (Sunnyvale,  
179 California, USA) equipped with a pulsed amperometric detector (PAD) with a disposable electrochemical gold electrode.  
180 Separation was achieved using a 4  $\times$  250 mm IonPac AS4A column (Dionex) connected to IonPac AG4A (4x50) guard  
181 column, operated at 30  $^{\circ}\text{C}$ . Samples were analyzed essentially as previously described <sup>14</sup>. In brief, the mobile phases were  
182 0.1 M sodium hydroxide (A) and 1 M sodium acetate in 0.1 M sodium hydroxide (B) and a linear gradient was developed  
183 from 1% B to 88.5% B over 100 minutes, i.e. 8.75 mM sodium acetate/min, at a flow rate of 1 mL/min. The PAD detector  
184 was set to use an AAA waveform for optimal signal-to-noise detection. Data acquisition and analysis were done using  
185 Chromeleon 7.2 (Thermo Scientific).

186 Enzymatic saccharification of *S. latissima*

187 Enzymatic saccharification of *S. latissima* was performed in reactions containing 15 % dry matter (DM) seaweed (grinded  
188 and then dried at 50  $^{\circ}\text{C}$ ; see Sharma and Horn [2016] for details) in seawater, which were incubated at 55 $^{\circ}\text{C}$  for 24 hours.  
189 The commercial enzyme preparations were Cellic CTec2 (Novozymes A/S, Denmark) and alginate lyase A1603 from Sigma  
190 Aldrich, Germany. AMOR\_PL7A was dosed according to its protein content and the amounts of protein dosed were similar  
191 to appropriate amounts of powdered commercial lyase that had previously been determined by <sup>9</sup>. Cellic CTec2 was dosed  
192 according to its protein content determined by the Bradford method <sup>38</sup> at 6.3 mg/g DM. The hydrolysates were subjected  
193 to rheological measurements without further processing.

194 Rheological measurements

195 The viscosity measurements were done with continuous rotation using an MCR301 rheometer from Anton Paar fitted with  
196 a PP50/P2 measuring system and a Peltier element ensuring a temperature of 20  $^{\circ}\text{C}$ . The shear rate was ramped during

197 the analysis from  $10\text{ s}^{-1}$  to  $200\text{ s}^{-1}$ . Amplitude sweep measurements were done using the same rheometer at a frequency  
198 of 1 Hz, changing the amplitude from 0.01% to 100% strain (i.e. relative change in length). The limit of the linear viscoelastic  
199 range was defined as the point where the storage modulus,  $G'$ , was reduced by 3%.

## 200 Results and discussion

### 201 Sequence analysis

202 The deduced amino acid sequence was subjected to dbCAN analysis <sup>22</sup>, leading to the identification of a putative PL7  
203 domain; the protein was therefore named AMOR\_PL7A (Figure S1). The presence of an N-terminal lipoanchor predicted  
204 by the LipoP server indicates that AMOR\_PL7A is most likely secreted and anchored to the cell membrane. Alignment of  
205 AMOR\_PL7A with available protein sequences from GenBank and the PDB showed that AMOR\_PL7A has the highest  
206 sequence identity (46%) to two putative endo alginate lyases from *Rhodopirellula sp.* SWK7 and *Vibrio hyugaensis*, both  
207 of which belong to species commonly found in salt water <sup>39, 40</sup>. The most similar protein with a known structure is an  
208 alginate lyase called A1-II' (PDB id: 2CWS) from *Sphingomonas sp.* A1 <sup>41</sup>, with 29 % identity (Figure S1) within 83 % of the  
209 sequence. Another related enzyme with known structure is PA1167 from *Pseudomonas aeruginosa* <sup>42</sup>(30% identity within  
210 62 % of the sequence; Figure S1). Candidate key catalytic residues in AMOR\_PL7A are His163 and Tyr256, which  
211 correspond to His191 and Tyr284 in A1-II' <sup>43</sup>. Additional active site residues previously shown to be crucial for A1-II' activity  
212 <sup>41</sup>, are also present in AMOR\_PL7A and include Arg118, Glu120, Arg122, Gln161 and Lys253 (Figure S1). Phylogenetic  
213 analysis (Fig. S3) showed that AMOR\_PL7A does not belong to one of the five best known subfamilies of PL7s that were  
214 described by Lombard et al <sup>44</sup>. The protein groups with PL7s from a variety of other, mostly marine, bacteria, including  
215 thermophiles.

216 AMOR\_PL7A was produced without its signal peptide and the cysteine putatively used for lipo-anchoring, and  
217 including a C-terminal His-tag (AHHHHHH). Typical yields of purified concentrated protein (Figure S2) were approximately  
218 60 mg per 500 mL culture broth.

## 219 Characterization of AMOR\_PL7A

220 The activity of AMOR\_PL7A was characterized using commercially available sodium alginate (Sigma Aldrich) and purified  
221 polyM, polyG and polyMG (see materials and methods for details). Initial incubations of alginate with AMOR\_PL7A resulted  
222 in increased absorbance at 235 nm, a clear indication of production of unsaturated oligosaccharides and thus alginate  
223 lyase activity<sup>45</sup>. Figures 1 and 2 show that AMOR\_PL7A has a broad activity range in terms of temperature, pH and salinity.  
224 At pH 6.0, the enzyme has highest activity at 65°C, and more than 60 % of this activity is maintained in the temperature  
225 range of 60 °C to 80 °C (Figure 1A). At 65 °C, AMOR\_PL7A has highest activity at pH 6.0, which is typical for alginate lyases  
226 of bacterial origin<sup>46</sup>, and 70 % of maximal activity is maintained in a wide pH range spanning from pH 4.8 to 7.8 (Figure  
227 1B). Figure 2 shows that AMOR\_PL7A is active in a broad salinity range from 0 to 2M of NaCl, and has highest activity in  
228 seawater. The high tolerance to salts and broad pH range are useful in seaweed processing since these properties allow  
229 direct treatment, without applying pre-processing steps such as removal of salts<sup>47</sup> or buffering<sup>48</sup>.

230 In the absence of substrate, the half-life of AMOR\_PL7A at 65°C, pH 6.0, was approximately three hours (Figure 3). The  
231 high stability of AMOR\_PL7A was confirmed by differential scanning calorimetry experiments which yielded apparent  
232 melting temperatures of approximately 71 °C both in buffer (pH 6.0) containing 500 mM NaCl and in pure seawater,  
233 whereas stability at lower salt concentrations (50 mM) was slightly reduced, but still high ( $T_{m,app} = 64.1$  °C) (Figure 4). To  
234 the best of our knowledge, AMOR\_PL7A is one of the most thermoactive and thermostable PL7s known to date. Only one  
235 PL7, the M-type alginate lyase from *Sphingomonas* sp., seems to have similar thermophilic properties, having a reported  
236 temperature optimum of 70 °C<sup>49</sup>, whereas other thermostable alginate lyases seem to operate optimally at lower  
237 temperatures<sup>11,50-52</sup>. The alginate lyase A1-II' shown in the alignment of Figure S1 lost the majority of its activity already  
238 after 10 minutes of incubation at 50°C<sup>49</sup>. The thermal tolerance of AMOR\_PL7A is a highly desired property when used in  
239 combination with other enzymes whose optimum temperatures are high, such as the cellulolytic enzyme cocktail Cellic  
240 CTec 2, which works most efficiently at around 50 °C<sup>53</sup>. Thus, the use of AMOR\_PL7A likely allows one-pot combined lyase-  
241 cellulase processing of seaweed biomass at high temperatures, as is shown below.

242 Using optimal conditions (pH 6.0, 500 mM NaCl, 65°C) steady state kinetic analysis of AMOR\_PL7A activity on sodium  
243 alginate (Figure S4) yielded a  $K_M$  of 0.51 +/- 0.09 mg/mL and a  $k_{cat}$  of 7.8 +/- 0.3 s<sup>-1</sup>. These values are in the same order of

244 magnitude as for other kinetically characterized alginate lyases (e.g. <sup>34,54</sup>). At 0.5% (w/v) substrate concentration,  
245 AMOR\_PL7A showed similar reducing-end liberating activities for sodium alginate and PolyM, whereas activity towards  
246 PolyG and PolyMG was very low (Figure 5). The progress curves in Figure 5 indicate specific activity on alginate in the order  
247 of 3.8  $\mu\text{mol}/\text{mg}\cdot\text{min}$ , whereas the initial specific activity towards PolyM may be up to three times higher. Clearly,  
248 AMOR\_PL7A is an M-specific alginate lyase.

249 Figure 6A shows that AMOR\_PL7A generates oligosaccharides from polyM with an unsaturated hexenuronic acid residue,  
250 4-deoxy-L-erythro-hex-4-ene-pyranosyluronate ( $\Delta$ ), at the non-reducing end and hence is a true alginate lyase. After one  
251 hour of degradation, oligomers of DP3-40 were observed in low amounts, whereas after 24 hours, there were only trace  
252 amounts left of oligomers with DP >5. Addition of fresh AMOR\_PL7A after 24 hours followed by incubation for another 24  
253 hours led to only minor additional degradation, reflected in a small reduction of  $\Delta\text{M5}$ . Using M12 and M24 as substrates,  
254 we observed a mixture of saturated and unsaturated products after 24h incubation (Figure 6B), confirming that the  
255 enzyme is endo-acting.

#### 256 Saccharification of brown seaweed (*Saccharina latissima*) at 55°C

257 The industrial applicability of AMOR\_PL7A was assessed in degradation of milled and dried *S. latissima* with the  
258 commercial cellulase cocktail Cellic Ctec2 at 55°C for 24 h in seawater (pH 6.8; no buffer added). Both AMOR\_PL7A and  
259 Cellic Ctec2 were expected to work at those conditions, whereas commercial alginate lyase from Sigma Aldrich has an  
260 optimal activity at lower temperature (37°C, according to the supplier's data sheet). Various enzyme combinations were  
261 compared based on their effectiveness in reducing viscosity and releasing glucose in reactions at an industrially relevant  
262 high-density solid loading (15 % DM). Inclusion of endo-type alginate lyases as such is not expected to directly improve  
263 glucose yield, but rather to make the reaction mixtures less viscous, thus likely increasing the efficiency of the cellulase  
264 cocktail. Figure 7A shows that inclusion of an alginate lyase leads to faster glucose release and about 25 % higher glucose  
265 yield at the final sampling point (24 h). Figure 7A also shows that AMOR\_PL7A is more efficient than the commercial  
266 alginate lyase and this difference became more pronounced in experiments with a 40 times lower enzyme dosage (0.0135  
267 mg/g rather than 0.7 mg/g lyase; Figure 7B). It is worth noting that, when using AMOR\_PL7A, the enzyme dose could be  
268 lowered by 40-times (to 0.0135 mg/g DM) without altering the final glucose yield (compare Figures 7A and 7B).

269 Characterization of rheological properties are important to understand the behavior of polysaccharides such as alginate,  
270 which even at low concentrations significantly increases the viscosity of a solution. A typical measurement from an  
271 industrial perspective is viscosity (Pas). To further assess the impact of AMOR\_PL7A on seaweed processing, we measured  
272 the viscosity of seaweed hydrolysates after 24 hours incubation at 55 °C in the absence and presence of an alginate lyase  
273 and Cellic Ctec2. Based on the rheological measurements, addition of an alginate lyase caused a large decrease in viscosity  
274 and AMOR\_PL7A worked better than the commercial enzyme (Figure 8). Treatment with Cellic Ctec2 did not reduce the  
275 viscosity relative to a reaction without any added enzyme. Although direct comparison of the two enzyme samples is  
276 complicated by lack of information for the commercial enzyme, these results show that AMOR\_PL7A is highly efficient for  
277 seaweed processing at higher temperatures. The AMOR\_PL7A + Cellic Ctec2 hydrolysate was found to be much softer  
278 (lower G'; Figure S5) and weaker (lower shear stress at limit of LVR; Figure S6), than the other hydrolysates.

279 In conclusion, AMOR\_PL7A, derived from the AMOR metagenomic dataset, is an M-specific alginate lyase (EC 4.2.2.3) that  
280 works optimally at 65 °C, pH 6.0, and has a broad tolerance to different NaCl concentrations. AMOR\_PL7A is one of the  
281 most thermostable alginate lyases known to date (e.g.<sup>11,50-52</sup>). The enzyme is easy to produce and more efficient than an  
282 available commercial alginate lyase at reaction temperatures that are typical for other enzymes used in biomass  
283 processing, such as the Cellic CTec2 cocktail. Indeed, addition of small amounts of AMOR\_PL7A improved glucose release  
284 from seaweed by Cellic CTec2 in terms of both speed and yield. This improvement was accompanied by a marked reduction  
285 in the viscosity of the reaction mixture. The present study adds to (a limited number of) previous studies on the effects of  
286 alginate lyases on saccharification by cellulase cocktails (<sup>9-11</sup>) by showing that AMOR\_PL7A allows running simultaneous  
287 cellulase-lyase reactions at temperatures and dry matter concentrations that are higher than those used previously.  
288 AMOR\_PL7A has the potential to increase the efficiency of enzymatic seaweed processing at large scale, not only because  
289 of the benefits of a fast reduction in viscosity (i.e. lower energy requirements for mixing and higher efficiency of other  
290 enzymes), but also because the enzyme works well in pure seawater, alleviating the need for additional chemicals or  
291 buffers.

292 It should be noted that the Cellic Ctec2 cocktail, used here as proof-of-principle, has been developed for conversion of  
293 lignocellulosic biomass. There are currently no commercial enzyme cocktails available for complete conversion of seaweed

294 to fermentable sugars. Since the market for seaweed-derived products and technologies for large-scale seaweed  
295 cultivations are expected to grow, there is a growing need for new enzyme cocktails designed specifically for seaweed  
296 processing. AMOR\_PL7A may become part of such cocktails.

## 297 298 Supporting information

299 Amino acid sequence alignment of the catalytic domain of AMOR\_PL7A with related PL7 alginate lyase domains with a  
300 known structure; SDS-PAGE analysis of purified AMOR\_PL7A; phylogenetic analysis of AMOR\_PL7A; steady state kinetics  
301 of AMOR\_PL7A; oscillatory measurements of seaweed hydrolysates treated with different enzymes.

## 302 303 Acknowledgements

304 This research was supported by the Research Council of Norway through grants 229003 (BIOFEED – Novel salmon feed  
305 by integrated bioprocessing of non-food biomass), 237841 (Foods of Norway) and 221568 (NorZymeD). Infrastructure  
306 was supported in part by NorBioLab grants 226247 and 270038 provided by the Research Council of Norway. The  
307 authors would like to thank Marianne Slang-Jensen for advice in the studies of protein stability.

- 311 (1) Haug, A.; Larsen, B.; Smidsrød, O. Uronic Acid Sequence in Alginate from Different Sources. *Carbohydr. Res.* **1974**,  
312 32 (2), 217–225. [https://doi.org/10.1016/S0008-6215\(00\)82100-X](https://doi.org/10.1016/S0008-6215(00)82100-X).
- 313 (2) Onsøyen, E. Alginates. In *Thickening and Gelling Agents for Food*; Springer US: ISBN 978-1-4615-2197-6, 1997; pp  
314 22–44. [https://doi.org/10.1007/978-1-4615-2197-6\\_2](https://doi.org/10.1007/978-1-4615-2197-6_2).
- 315 (3) Stévant, P.; Rebours, C.; Chapman, A. Seaweed Aquaculture in Norway: Recent Industrial Developments and  
316 Future Perspectives. *Aquac. Int.* **2017**, 25 (4), 1373–1390. <https://doi.org/10.1007/s10499-017-0120-7>.
- 317 (4) Handå, A.; Forbord, S.; Wang, X.; Broch, O. J.; Dahle, S. W.; Størseth, T. R.; Reitan, K. I.; Olsen, Y.; Skjermo, J.  
318 Seasonal- and Depth-Dependent Growth of Cultivated Kelp (*Saccharina Latissima*) in Close Proximity to Salmon  
319 (*Salmo Salar*) Aquaculture in Norway. *Aquaculture* **2013**, 414–415 (414–415), 191–201.  
320 <https://doi.org/10.1016/j.aquaculture.2013.08.006>.
- 321 (5) Schiener, P.; Black, K. D.; Stanley, M. S.; Green, D. H. The Seasonal Variation in the Chemical Composition of the  
322 Kelp Species *Laminaria Digitata*, *Laminaria Hyperborea*, *Saccharina Latissima* and *Alaria Esculenta*. *J. Appl. Phycol.*  
323 **2015**, 27 (1), 363–373. <https://doi.org/10.1007/s10811-014-0327-1>.
- 324 (6) Enquist-Newman, M.; Faust, A. M. E.; Bravo, D. D.; Santos, C. N. S.; Raisner, R. M.; Hanel, A.; Sarvabhowman, P.;  
325 Le, C.; Regitsky, D. D.; Cooper, S. R.; et al. Efficient Ethanol Production from Brown Macroalgae Sugars by a  
326 Synthetic Yeast Platform. *Nature* **2014**, 505 (7482), 239–243. <https://doi.org/10.1038/nature12771>.
- 327 (7) Wargacki, A. J.; Leonard, E.; Win, M. N.; Regitsky, D. D.; Santos, C. N. S.; Kim, P. B.; Cooper, S. R.; Raisner, R. M.;  
328 Herman, A.; Sivitz, A. B.; et al. An Engineered Microbial Platform for Direct Biofuel Production from Brown  
329 Macroalgae. *Science (80-. )* **2012**, 335 (6066), 308–313. <https://doi.org/10.1126/science.1214547>.
- 330 (8) Sharma, S.; Hansen, L. D.; Hansen, J. O.; Mydland, L. T.; Horn, S. J.; Øverland, M.; Eijsink, V. G. H.; Vuoristo, K. S.  
331 Microbial Protein Produced from Brown Seaweed and Spruce Wood as a Feed Ingredient. *J. Agric. Food Chem.*  
332 **2018**, acs.jafc.8b01835. <https://doi.org/10.1021/acs.jafc.8b01835>.
- 333 (9) Sharma, S.; Horn, S. J. Enzymatic Saccharification of Brown Seaweed for Production of Fermentable Sugars.  
334 *Bioresour. Technol.* **2016**, 213, 155–161. <https://doi.org/10.1016/j.biortech.2016.02.090>.
- 335 (10) Ravanal, M. C.; Sharma, S.; Gimpel, J.; Reveco-Urzuá, F. E.; Øverland, M.; Horn, S. J.; Lienqueo, M. E. The Role of  
336 Alginate Lyases in the Enzymatic Saccharification of Brown Macroalgae, *Macrocystis Pyrifera* and *Saccharina*  
337 *Latissima*. *Algal Res.* **2017**, 26, 287–293. <https://doi.org/10.1016/J.ALGAL.2017.08.012>.
- 338 (11) Manns, D.; Andersen, S. K.; Saake, B.; Meyer, A. S. Brown Seaweed Processing: Enzymatic Saccharification of  
339 *Laminaria Digitata* Requires No Pre-Treatment. *J. Appl. Phycol.* **2016**, 28 (2), 1287–1294.  
340 <https://doi.org/10.1007/s10811-015-0663-9>.
- 341 (12) Ertesvåg, H. Alginate-Modifying Enzymes: Biological Roles and Biotechnological Uses. *Front. Microbiol.* **2015**, 6,  
342 523. <https://doi.org/10.3389/fmicb.2015.00523>.
- 343 (13) Gacesa, P. Alginate-Modifying Enzymes: A Proposed Unified Mechanism of Action for the Lyases and Epimerases.  
344 *FEBS Lett.* **1987**, 212 (2), 199–202. [https://doi.org/10.1016/0014-5793\(87\)81344-3](https://doi.org/10.1016/0014-5793(87)81344-3).
- 345 (14) Aarstad, O. A.; Tøndervik, A.; Sletta, H.; Skjåk-Bræk, G. Alginate Sequencing: An Analysis of Block Distribution in  
346 Alginates Using Specific Alginate Degrading Enzymes. *Biomacromolecules* **2012**, 13 (1), 106–116.  
347 <https://doi.org/10.1021/bm2013026>.
- 348 (15) Rødsrud, G.; Lersch, M.; Sjöde, A. Biomass and Bioenergy. *Biomass and Bioenergy* **2012**, 46, 46–59.
- 349 (16) Sjöde, A.; Frölander, A.; Lersch, M.; Rødsrud, G. Lignocellulosic Biomass Conversion by Sulfite Pretreatment.  
350 Patent EP2376642B1 December 16, 2013, p 23.
- 351 (17) Pedersen, R. B.; Thorseth, I. H.; Hellevang, B.; Schultz, A.; Taylor, P.; Knudsen, H. P.; Steinsbu, B. O. Two Vent  
352 Fields Discovered at the Ultraslow Spreading Arctic Ridge System. *EOS Trans. Am. Geophys. Union, Fall Meet.*

- 353 *Suppl., Abstr. OS21C-01 2005, 86 (52).*
- 354 (18) Schander, C.; Rapp, H. T.; Kongsrud, J. A.; Bakken, T.; Berge, J.; Cochrane, S.; Oug, E.; Byrkjedal, I.; Todt, C.;  
355 Cedhagen, T.; et al. The Fauna of Hydrothermal Vents on the Mohn Ridge (North Atlantic). *Mar. Biol. Res.* **2010**, *6*  
356 (2), 155–171. <https://doi.org/10.1080/17451000903147450>.
- 357 (19) Fredriksen, L.; Stokke, R.; Jensen, M. S.; Westereng, B.; Jameson, J.-K.; Steen, I. H.; Eijsink, V. G. H. Discovery of a  
358 Thermostable GH10 Xylanase with Broad Substrate Specificity from the Arctic Mid-Ocean Ridge Vent System.  
359 *Appl. Environ. Microbiol.* **2019**, AEM.02970-18. <https://doi.org/10.1128/AEM.02970-18>.
- 360 (20) Hyatt, D.; LoCascio, P. F.; Hauser, L. J.; Uberbacher, E. C. Gene and Translation Initiation Site Prediction in  
361 Metagenomic Sequences. *Bioinformatics* **2012**, *28* (17), 2223–2230.  
362 <https://doi.org/10.1093/bioinformatics/bts429>.
- 363 (21) Hyatt, D.; Chen, G.-L.; LoCascio, P. F.; Land, M. L.; Larimer, F. W.; Hauser, L. J. Prodigal: Prokaryotic Gene  
364 Recognition and Translation Initiation Site Identification. *BMC Bioinformatics* **2010**, *11* (1), 119.  
365 <https://doi.org/10.1186/1471-2105-11-119>.
- 366 (22) Yin, Y.; Mao, X.; Yang, J.; Chen, X.; Mao, F.; Xu, Y. DbCAN: A Web Resource for Automated Carbohydrate-Active  
367 Enzyme Annotation. *Nucleic Acids Res.* **2012**, *40* (W1), W445–W451. <https://doi.org/10.1093/nar/gks479>.
- 368 (23) Kelley, L. A.; Mezulis, S.; Yates, C. M.; Wass, M. N.; Sternberg, M. J. E. The Phyre2 Web Portal for Protein  
369 Modeling, Prediction and Analysis. *Nat. Protoc.* **2015**, *10* (6), 845–858. <https://doi.org/10.1038/nprot.2015.053>.
- 370 (24) Juncker, A. S.; Willenbrock, H.; von Heijne, G.; Brunak, S.; Nielsen, H.; Krogh, A. Prediction of Lipoprotein Signal  
371 Peptides in Gram-Negative Bacteria. *Protein Sci.* **2003**, *12* (8), 1652–1662. <https://doi.org/10.1110/ps.0303703>.
- 372 (25) Kumar, S.; Stecher, G.; Tamura, K. MEGA7: Molecular Evolutionary Genetics Analysis Version 7.0 for Bigger  
373 Datasets. *Mol. Biol. Evol.* **2016**, *33* (7), 1870–1874. <https://doi.org/10.1093/molbev/msw054>.
- 374 (26) Edgar, R. C. MUSCLE: Multiple Sequence Alignment with High Accuracy and High Throughput. *Nucleic Acids Res.*  
375 **2004**, *32* (5), 1792–1797. <https://doi.org/10.1093/nar/gkh340>.
- 376 (27) Gouet, P.; Courcelle, E.; Stuart, D. I.; Métoz, F. ESPript: Analysis of Multiple Sequence Alignments in PostScript.  
377 *Bioinformatics* **1999**, *15* (4), 305–308.
- 378 (28) Potter, S. C.; Luciani, A.; Eddy, S. R.; Park, Y.; Lopez, R.; Finn, R. D. HMMER Web Server: 2018 Update. *Nucleic*  
379 *Acids Res.* **2018**, *46* (W1), W200–W204. <https://doi.org/10.1093/nar/gky448>.
- 380 (29) Katoh, K.; Standley, D. M. MAFFT Multiple Sequence Alignment Software Version 7: Improvements in  
381 Performance and Usability. *Mol. Biol. Evol.* **2013**, *30* (4), 772–780. <https://doi.org/10.1093/molbev/mst010>.
- 382 (30) Katoh, K.; Misawa, K.; Kuma, K.; Miyata, T. MAFFT: A Novel Method for Rapid Multiple Sequence Alignment Based  
383 on Fast Fourier Transform. *Nucleic Acids Res.* **2002**, *30* (14), 3059–3066.
- 384 (31) Nguyen, L.-T.; Schmidt, H. A.; von Haeseler, A.; Minh, B. Q. IQ-TREE: A Fast and Effective Stochastic Algorithm for  
385 Estimating Maximum-Likelihood Phylogenies. *Mol. Biol. Evol.* **2015**, *32* (1), 268–274.  
386 <https://doi.org/10.1093/molbev/msu300>.
- 387 (32) Aslanidis, C.; de Jong, P. J. Ligation-Independent Cloning of PCR Products (LIC-PCR). *Nucleic Acids Res.* **1990**, *18*  
388 (20), 6069–6074. <https://doi.org/10.1093/nar/18.20.6069>.
- 389 (33) Miller, G. L. Use of Dinitrosalicylic Acid Reagent for Determination of Reducing Sugar. *Anal. Chem.* **1959**, *31* (3),  
390 426–428. <https://doi.org/10.1021/ac60147a030>.
- 391 (34) Swift, S. M.; Hudgens, J. W.; Heselpoth, R. D.; Bales, P. M.; Nelson, D. C. Characterization of AlgMsp, an Alginate  
392 Lyase from *Microbulbifer* Sp. 6532A. *PLoS One* **2014**, *9* (11), e112939.  
393 <https://doi.org/10.1371/journal.pone.0112939>.
- 394 (35) Preiss, J.; Ashwell, G. Alginic Acid Metabolism in Bacteria. I. Enzymatic Formation of Unsaturated  
395 Oligosaccharides and 4-Deoxy-L-Erythro-5-Hexoseulose Uronic Acid. *J. Biol. Chem.* **1962**, *237* (2), 309–316.



- 396 (36) Gimmestad, M.; Sletta, H.; Ertesvåg, H.; Bakkevig, K.; Jain, S.; Suh, S.; Skjåk-Braek, G.; Ellingsen, T. E.; Ohman, D.  
397 E.; Valla, S. The *Pseudomonas Fluorescens* AlgG Protein, but Not Its Mannuronan C-5-Epimerase Activity, Is  
398 Needed for Alginate Polymer Formation. *J. Bacteriol.* **2003**, *185* (12), 3515–3523.
- 399 (37) Donati, I.; Holtan, S.; Mørch, Y. A.; Borgogna, M.; Dentini, M.; Skjåk-Braek, G. New Hypothesis on the Role of  
400 Alternating Sequences in Calcium–Alginate Gels. *Biomacromolecules* **2005**, *6* (2), 1031–1040.  
401 <https://doi.org/10.1021/bm049306e>.
- 402 (38) Bradford, M. M. A Rapid and Sensitive Method for the Quantitation of Microgram Quantities of Protein Utilizing  
403 the Principle of Protein-Dye Binding. *Anal. Biochem.* **1976**, *72* (1–2), 248–254. [https://doi.org/10.1016/0003-  
404 2697\(76\)90527-3](https://doi.org/10.1016/0003-2697(76)90527-3).
- 405 (39) Winkelmann, N.; Jaekel, U.; Meyer, C.; Serrano, W.; Rachel, R.; Rossello-Mora, R.; Harder, J. Determination of the  
406 Diversity of Rhodospirillum Isolates from European Seas by Multilocus Sequence Analysis. *Appl. Environ.*  
407 *Microbiol.* **2010**, *76* (3), 776–785. <https://doi.org/10.1128/AEM.01525-09>.
- 408 (40) Urbanczyk, Y.; Ogura, Y.; Hayashi, T.; Urbanczyk, H. Description of a Novel Marine Bacterium, *Vibrio Hyugaensis*  
409 Sp. Nov., Based on Genomic and Phenotypic Characterization. *Syst. Appl. Microbiol.* **2015**, *38* (5), 300–304.  
410 <https://doi.org/10.1016/j.syapm.2015.04.001>.
- 411 (41) Yamasaki, M.; Ogura, K.; Hashimoto, W.; Mikami, B.; Murata, K. A Structural Basis for Depolymerization of  
412 Alginate by Polysaccharide Lyase Family-7. *J. Mol. Biol.* **2005**, *352* (1), 11–21.  
413 <https://doi.org/10.1016/j.jmb.2005.06.075>.
- 414 (42) Yamasaki, M.; Moriwaki, S.; Miyake, O.; Hashimoto, W.; Murata, K.; Mikami, B. Structure and Function of a  
415 Hypothetical *Pseudomonas Aeruginosa* Protein PA1167 Classified into Family PL-7. *J. Biol. Chem.* **2004**, *279* (30),  
416 31863–31872. <https://doi.org/10.1074/jbc.M402466200>.
- 417 (43) Ogura, K.; Yamasaki, M.; Mikami, B.; Hashimoto, W.; Murata, K. Substrate Recognition by Family 7 Alginate Lyase  
418 from *Sphingomonas* Sp. A1. *J. Mol. Biol.* **2008**, *380* (2), 373–385. <https://doi.org/10.1016/j.jmb.2008.05.008>.
- 419 (44) Lombard, V.; Bernard, T.; Rancurel, C.; Brumer, H.; Coutinho, P. M.; Henrissat, B. A Hierarchical Classification of  
420 Polysaccharide Lyases for Glycogenomics. *Biochem. J.* **2010**, *432* (3), 437–444.  
421 <https://doi.org/10.1042/BJ20101185>.
- 422 (45) Ostgaard, K. Determination of Alginate Composition by a Simple Enzymatic Assay. *Hydrobiologia* **1993**, *260–261*  
423 (1), 513–520. <https://doi.org/10.1007/BF00049064>.
- 424 (46) Wong, T. Y.; Preston, L. A.; Schiller, N. L. Alginate Lyase: Review of Major Sources and Enzyme Characteristics,  
425 Structure-Function Analysis, Biological Roles, and Applications. *Annu. Rev. Microbiol.* **2000**, *54* (1), 289–340.  
426 <https://doi.org/10.1146/annurev.micro.54.1.289>.
- 427 (47) Sterner, M.; Edlund, U. Multicomponent Fractionation Of *Saccharina Latissimabrown* Algae Using Chelating Salt  
428 Solutions. *J. Appl. Phycol.* **2016**, *28*, 2561–2574. <https://doi.org/10.1007/s10811-015-0785-0>.
- 429 (48) Ravanal, M. C.; Pezoa-Conte, R.; von Schoultz, S.; Hemming, J.; Salazar, O.; Anugwom, I.; Jogunola, O.; Mäki-  
430 Arvela, P.; Willför, S.; Mikkola, J.-P.; et al. Comparison of Different Types of Pretreatment and Enzymatic  
431 Saccharification of *Macrocystis Pyrifera* for the Production of Biofuel. *Algal Res.* **2016**, *13*, 141–147.  
432 <https://doi.org/10.1016/j.algal.2015.11.023>.
- 433 (49) Yoon, H.-J.; Hashimoto, W.; Miyake, O.; Okamoto, M.; Mikami, B.; Murata, K. Overexpression in *Escherichia Coli*,  
434 Purification, and Characterization of *Sphingomonas* Sp. A1 Alginate Lyases. *Protein Expr. Purif.* **2000**, *19* (1), 84–  
435 90. <https://doi.org/10.1006/prep.2000.1226>.
- 436 (50) Inoue, A.; Anraku, M.; Nakagawa, S.; Ojima, T. Discovery of a Novel Alginate Lyase from *Nitratiruptor* Sp. SB155-2  
437 Thriving at Deep-Sea Hydrothermal Vents and Identification of the Residues Responsible for Its Heat Stability \*  
438 Downloaded From. *J. Biol. Chem.* **2016**, *291* (30), 15551–15563. <https://doi.org/10.1074/jbc.M115.713230>.
- 439 (51) Li, H.; Wang, S.; Zhang, Y.; Chen, L.; Li, H.; Wang, S.; Zhang, Y.; Chen, L. High-Level Expression of a Thermally  
440 Stable Alginate Lyase Using *Pichia Pastoris*, Characterization and Application in Producing Brown Alginate

- 441 Oligosaccharide. *Mar. Drugs* **2018**, *16* (5), 158. <https://doi.org/10.3390/md16050158>.
- 442 (52) Zhu, B.; Ning, L.; Jiang, Y.; Ge, L. Biochemical Characterization and Degradation Pattern of a Novel Endo-Type  
443 Bifunctional Alginate Lyase AlyA from Marine Bacterium *Isoptericola Halotolerans*. *Mar. Drugs* **2018**, *16* (8).  
444 <https://doi.org/10.3390/md16080258>.
- 445 (53) Rodrigues, A. C.; Haven, M. Ø.; Lindedam, J.; Felby, C.; Gama, M. Celluclast and Cellic® CTec2:  
446 Saccharification/Fermentation of Wheat Straw, Solid–liquid Partition and Potential of Enzyme Recycling by  
447 Alkaline Washing. *Enzyme Microb. Technol.* **2015**, *79–80*, 70–77.  
448 <https://doi.org/10.1016/J.ENZMICTEC.2015.06.019>.
- 449 (54) Badur, A. H.; Jagtap, S. S.; Yalamanchili, G.; Lee, J. K.; Zhao, H.; Rao, C. V. Alginate Lyases from Alginate-Degrading  
450 *Vibrio Splendidus* 12B01 Are Endolytic. *Appl. Environ. Microbiol.* **2015**, *81* (5), 1865–1873.  
451 <https://doi.org/10.1128/AEM.03460-14>.
- 452
- 453

## 454 Figure legends

455 **Figure 1. Effect of temperature and pH on the activity of AMOR\_PL7A.** Experiments were conducted in triplicate and  
456 activity was determined by recording initial catalytic velocity. The reactions were incubated up to 50 minutes. Reactions  
457 giving non-linear progress curves, which implies that only a few early sampling points could be used to estimate activity,  
458 are indicated by an asterisk. Activity was normalized to 100% for the most active sample. The temperature optimum was  
459 determined using 50 mM sodium acetate buffer, pH 6.0; the pH optimum was determined at 65 °C.

460 **Figure 2. Salt tolerance of AMOR\_PL7A at 65°C, pH 6.0.** A reaction in seawater (no buffer or added salts) was also  
461 performed. The displayed activities reflect initial velocities, derived from a linear increase in absorbance at 235 nm during  
462 a 50-minute incubation at 65°C.

463 **Figure 3. Stability of AMOR\_PL7A at 65 °C.** AMOR\_PL7 (0.1 μM) was pre-incubated at 65 °C in 50 mM Tris-HCl, pH 6.0,  
464 with 500 mM NaCl without substrate for 0 to 24 hours, followed by assessment of remaining enzyme activity (initial  
465 velocity) at 65 °C. All reactions were carried out in triplicate and activity was normalized to 100% for the most active  
466 sample. Note that the presence of substrate stabilizes the enzyme as shown by the linearity of progress curves obtained  
467 under standard assay conditions, at 65 °C.

468 **Figure 4. Stability of AMOR\_PL7A assessed by Differential Scanning Calorimetry (DSC).** The graph shows DSC  
469 thermograms for AMOR-PL7 (1.3 mg/mL) in 50 mM NaOAc, pH 6.0, 50 mM NaCl (dashed line, apparent  $T_m$ ,  $T_{m,app} = 64.1^\circ\text{C}$ ),  
470 50 mM NaOAc, pH 6.0, 500 mM NaCl (dotted line,  $T_{m,app} = 71.5^\circ\text{C}$ ) NaCl, and unbuffered seawater (solid line,  $T_{m,app} =$   
471  $70.5^\circ\text{C}$ ). The protein samples were heated at a rate of  $1^\circ\text{C}/\text{min}$  and protein unfolding was irreversible.

472 **Figure 5. Reducing end formation (mM/mL) from sodium alginate, polyM, polyG and polyMG.** The reaction mixtures  
473 contained 12.7 nM of AMOR\_PL7A and 5 mg/mL of substrate in Tris HCl, pH 6.0, containing 250 mM NaCl and were  
474 incubated at 65 °C. The reactions were carried out in triplicates and the values presented represent the mean  $\pm$  standard  
475 deviation.

476 **Figure 6. Degradation of polyM by AMOR\_PL7A.** Panel A shows products generated from polyM after 0h, 1h, 4h, 24h  
477 incubation in seawater, at 65°C. “24 + 24h” represents a sample where fresh enzyme was added after 24 hours, followed  
478 by another 24 h incubation. The major peaks correspond to M-chains of varying DP with an unsaturated non-reducing  
479 end, i.e. a 4-deoxy-L-erythro-hex-4-enepyranosyluronate, denoted  $\Delta$ . Panel B shows products obtained upon 1) acid  
480 hydrolysis of PolyM, 2) degradation of PolyM using a previously characterized M-lyase from *Haliotis tuberculata*<sup>14</sup>, and  
481 degradation of 3) M12 and 4) M24 by AMOR\_PL7 in seawater at 65°C for 24h. Reactions 3 and 4 show mixtures of saturated  
482 and unsaturated products.

483 **Figure 7. Enzymatic release of glucose.** The graphs show release of glucose from *S. latissima* at 15 % solid loading, in  
484 seawater, at 55 °C. The enzyme doses were 6.3 mg for Cellic Ctec2 and 0.7 mg (A) or 0.0175 mg (B) of AMOR\_PL7A or the  
485 commercial alginate lyase (Sigma) per g DM. The reactions were carried out in triplicates and the values presented  
486 represent the mean  $\pm$  standard deviation.

487 **Figure 8. Viscosity (Pas) of hydrolyzed seaweed at different shear rates (1/s).** Viscosity was measured after 24 hours  
488 incubation of *S. latissima* (15 % DM) in seawater at 55°C with no added enzymes (Control), and with 6.3 mg per g DM  
489 Cellic Ctec2 in the absence of an alginate lyase or in the presence of 0.7 mg per g DM Sigma Aly or AMOR\_PL7A.

490

491

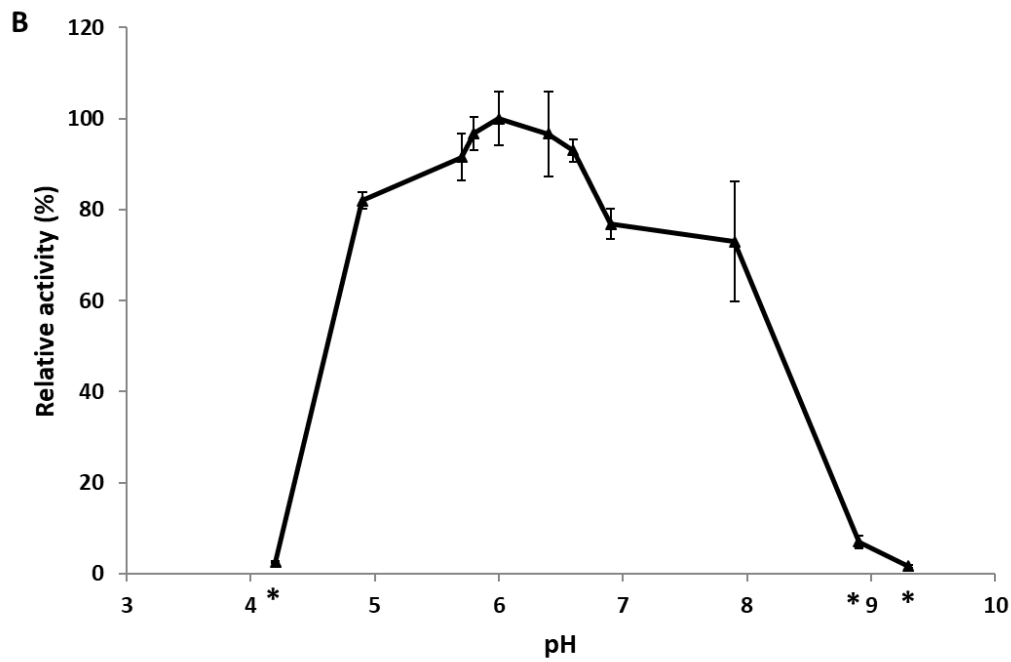
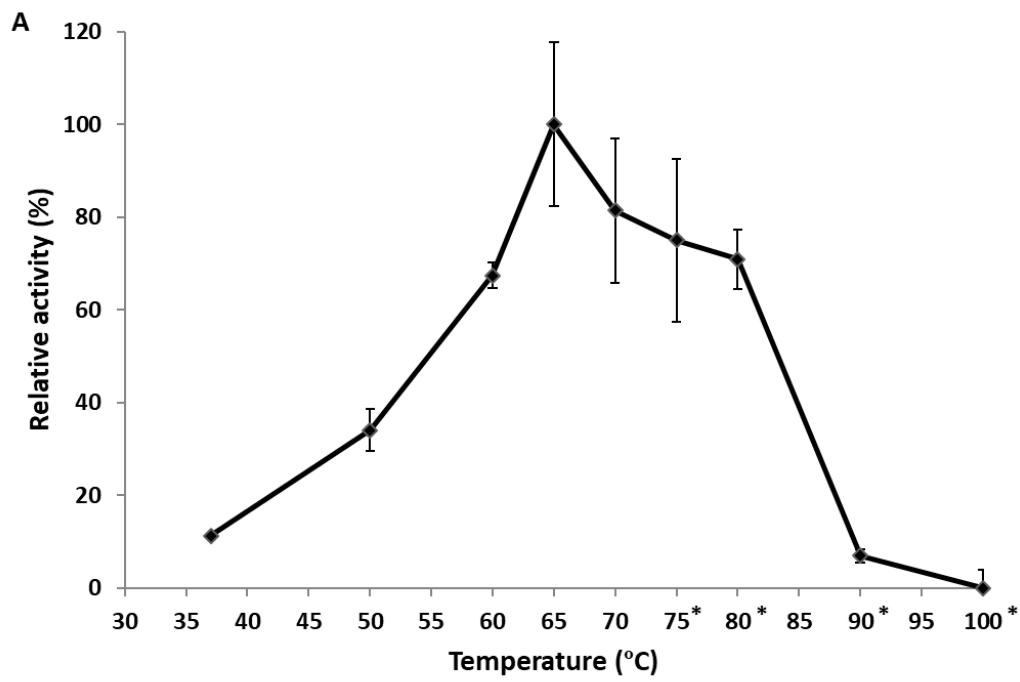


Figure 1 Effect of temperature and pH on the activity of AMOR\_PL7A.

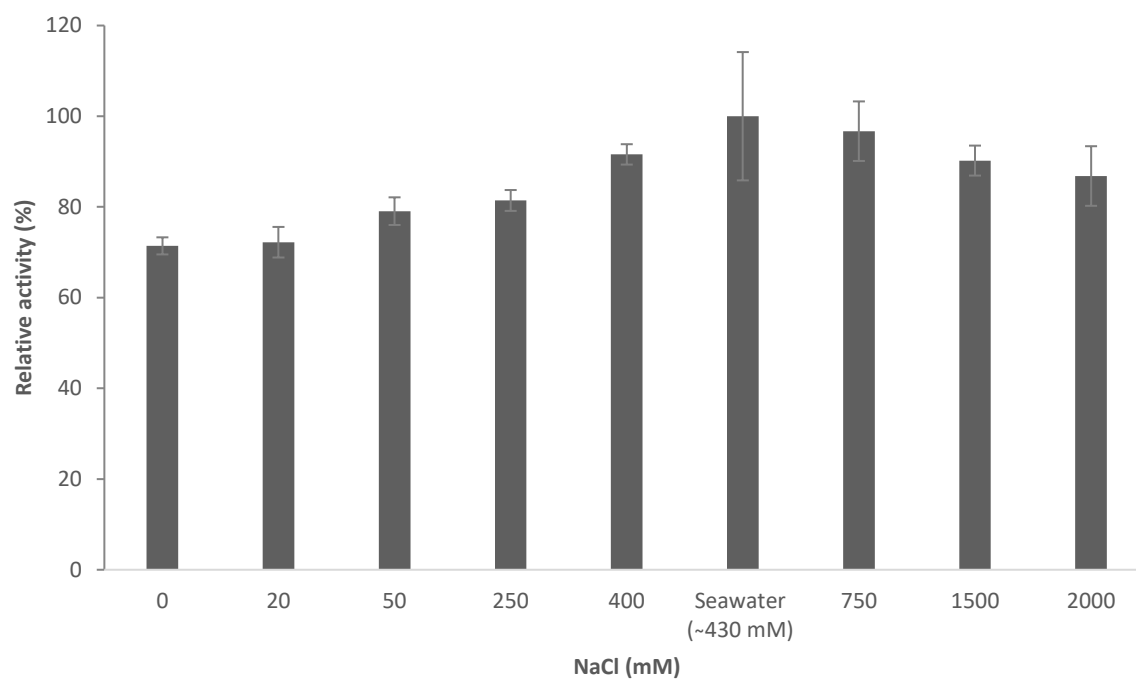


Figure 2 Salt tolerance of AMOR\_PL7A at 65°C, pH 6.0.

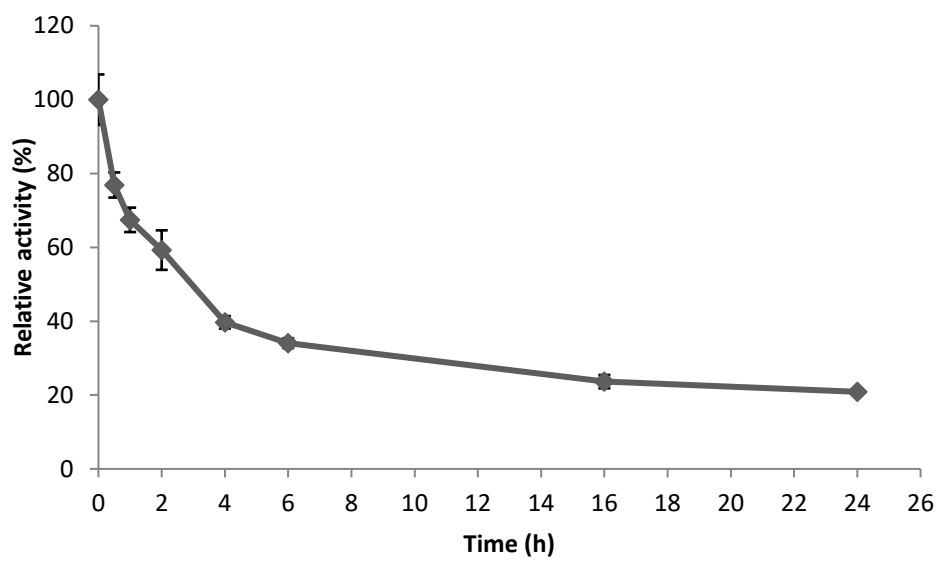


Figure 3 Stability of AMOR\_PL7A at 65 °C.

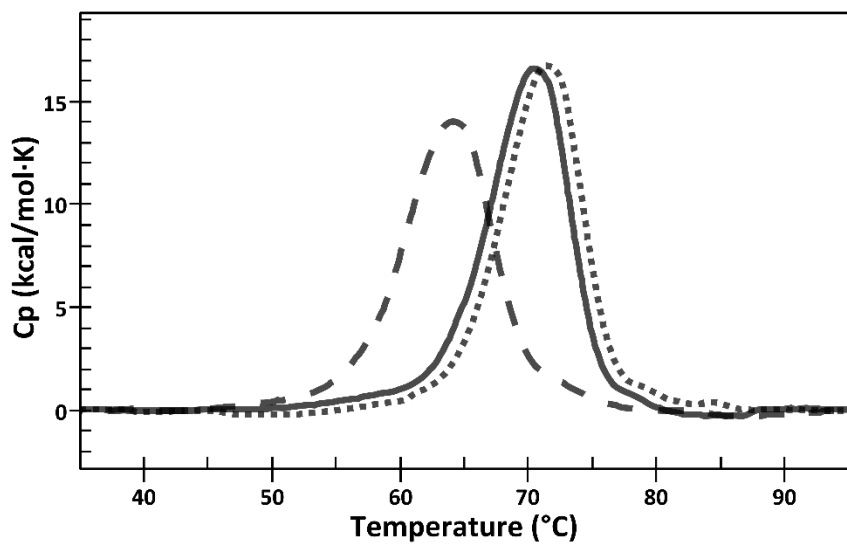


Figure 4 Stability of AMOR\_PL7A assessed by Differential Scanning Calorimetry (DSC).



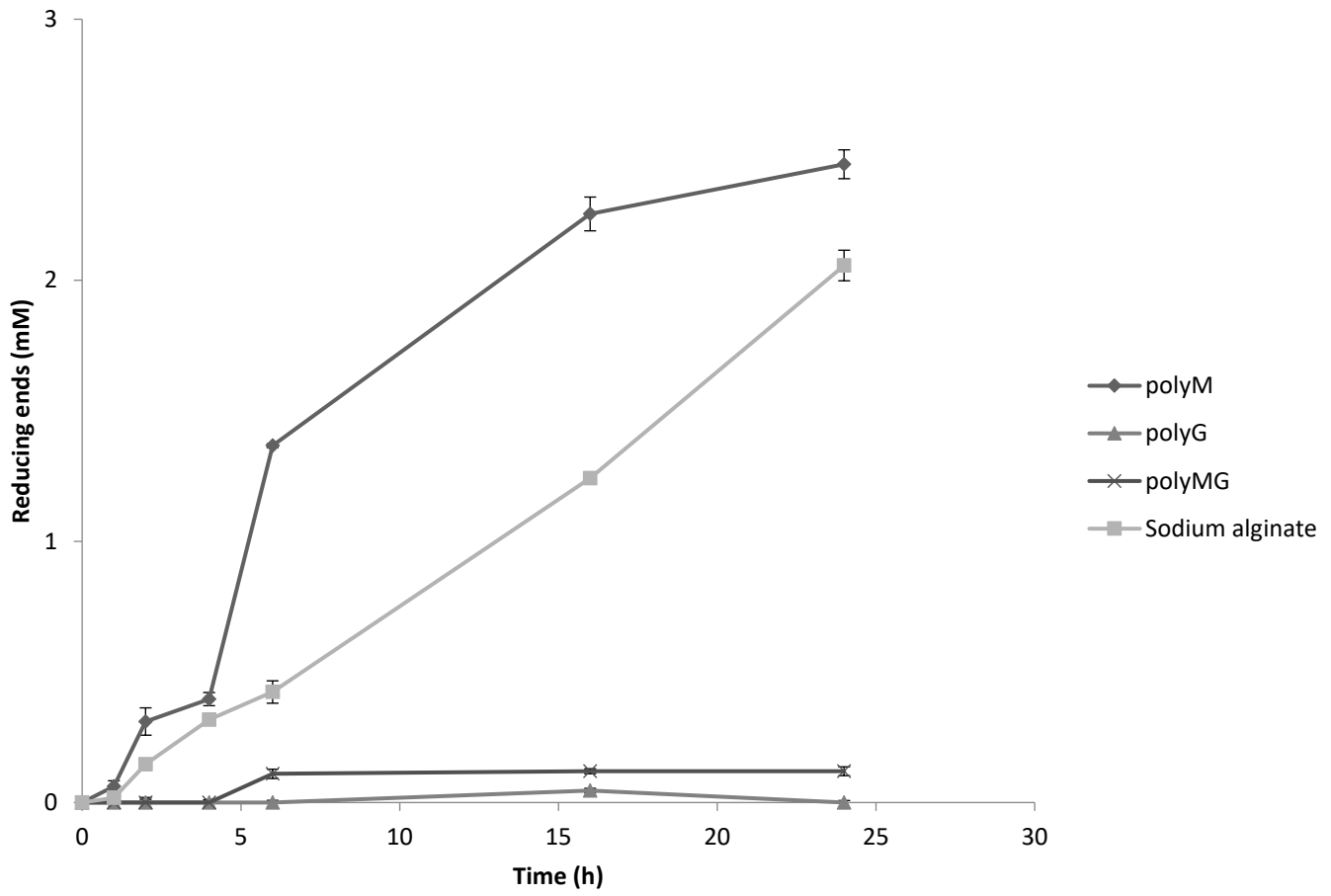


Figure 5 Reducing end formation (mM/mL) from sodium alginate, polyM, polyG and polyMG.

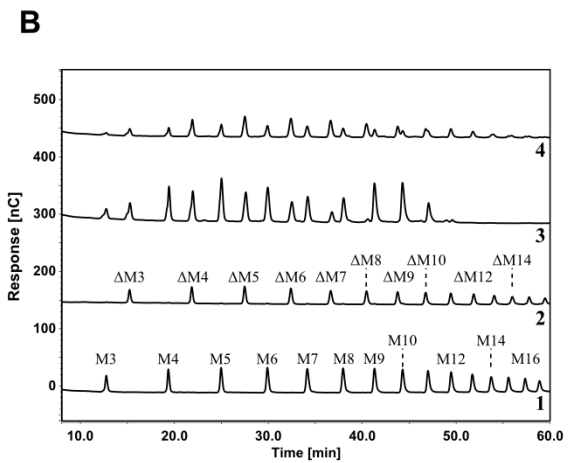
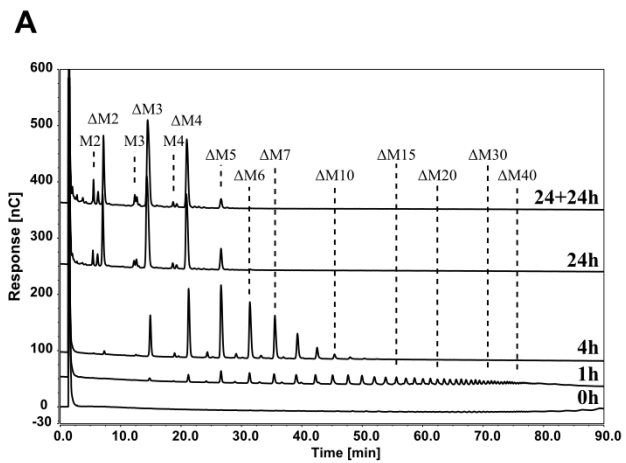
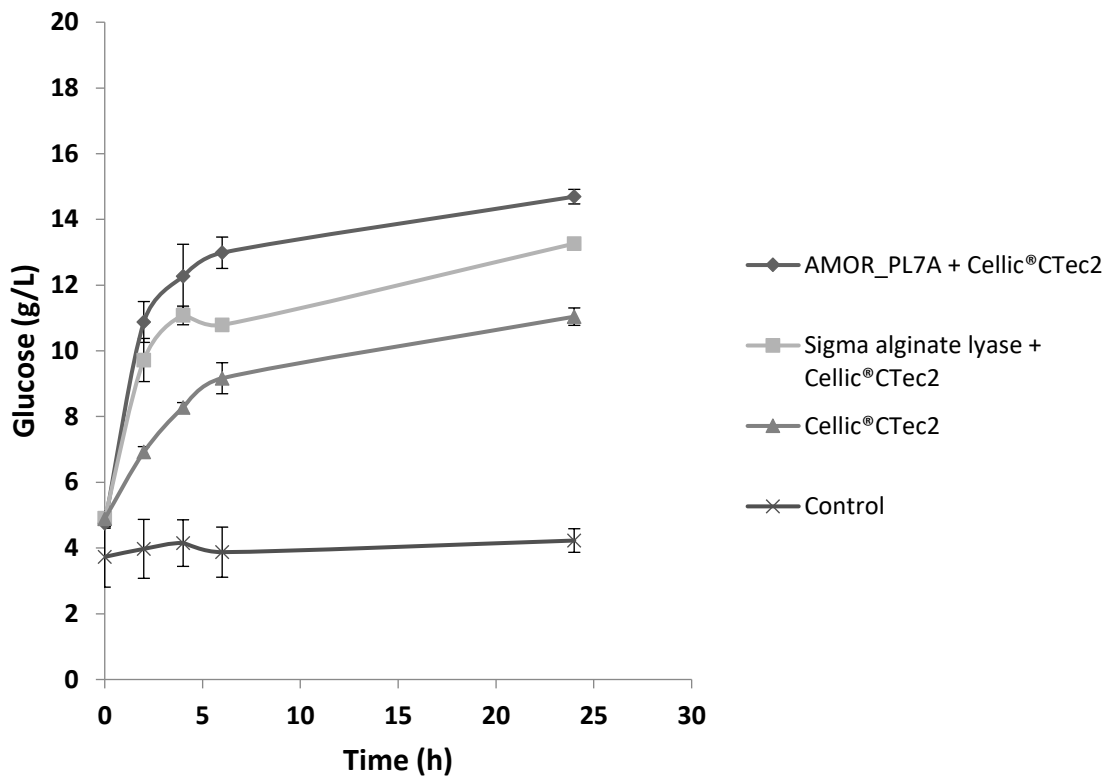


Figure 6 Degradation of polyM by AMOR\_PL7A.

**A**



# B

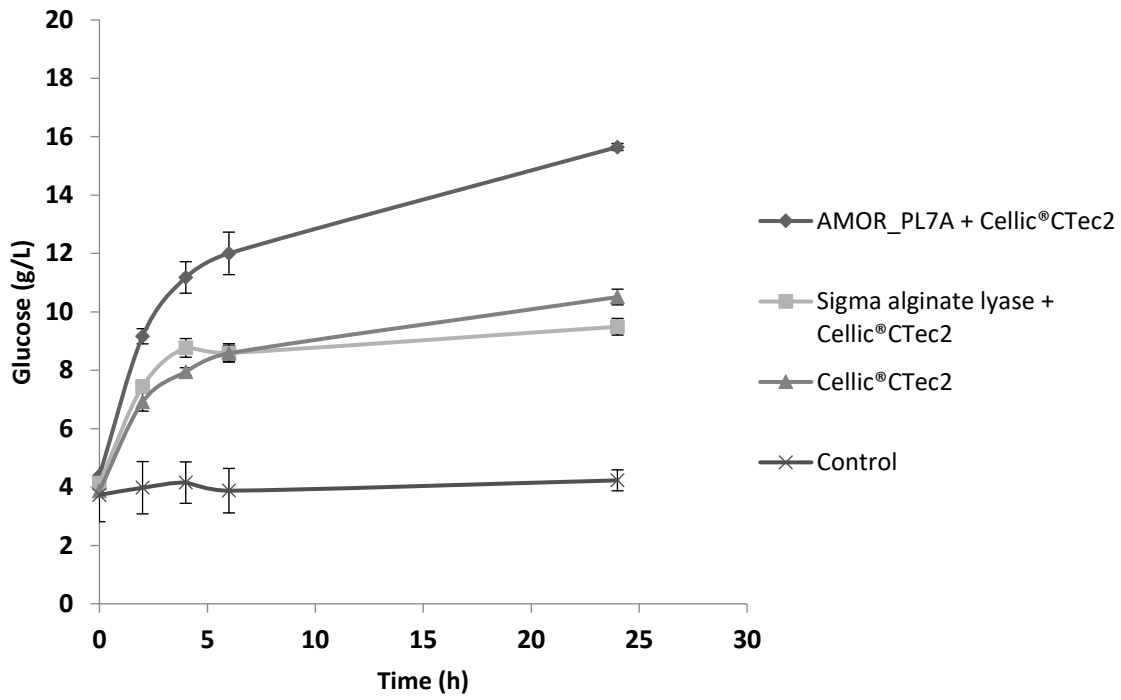


Figure 7 Enzymatic release of glucose.

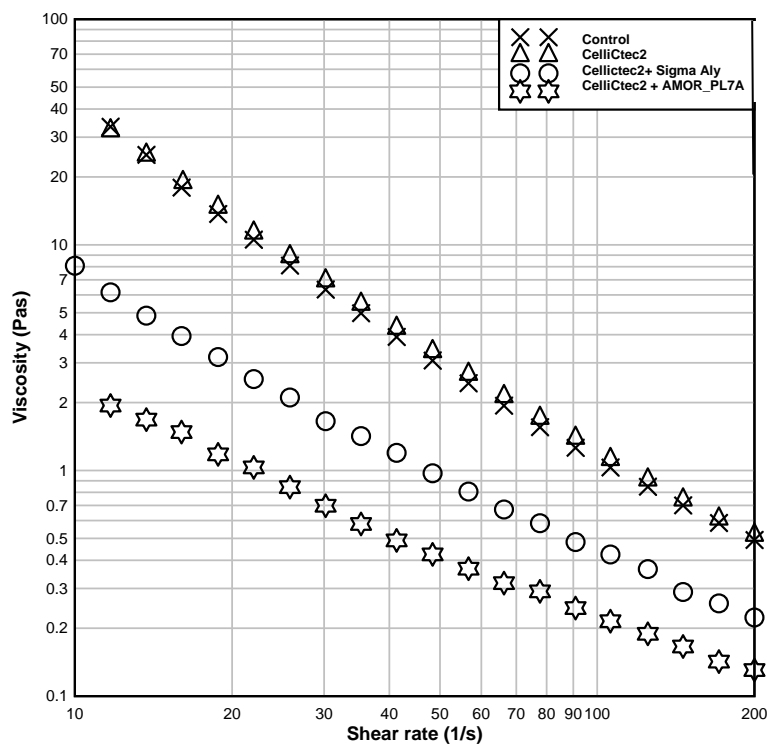


Figure 8 Viscosity (Pas) of hydrolyzed seaweed at different shear rates (1/s).

## Toc graphic

